Published in final edited form as:
Mol Pharm. 2010 August 2; 7(4): 1108–1117. doi:10.1021/mp900284c.

Interfacial Activity Assisted Surface Functionalization: A Novel Approach to Incorporate Maleimide Functional Groups and cRGD Peptide on Polymeric Nanoparticles for Targeted Drug Delivery

Udaya S. Toti[1], **Bharath Raja Guru**[1], **Alex E. Grill**[1], and **Jayanth Panyam**[1,2,*]

[1] Department of Pharmaceutics, College of Pharmacy, University of Minnesota, Minneapolis, MN 55455

[2] Masonic Cancer Center, University of Minnesota, Minneapolis, MN 55455

Abstract

Nanoparticles formulated using poly(D,L-lactide-*co*-glycolide) (PLGA) copolymer have emerged as promising carriers for targeted delivery of a wide variety of payloads. However, an important drawback with PLGA nanoparticles is the limited types of functional groups available on the surface for conjugation to targeting ligands. In the current report, we demonstrate that the Interfacial Activity Assisted Surface Functionalization (IAASF) technique can be used to incorporate reactive functional groups such as maleimide onto the surface of PLGA nanoparticles. The surface maleimide groups were used to conjugate cRGD peptide to nanoparticles. The cRGD peptide targets $\alpha_v\beta_3$ integrins overexpressed on tumor vasculature and some tumor cells, and was used as model targeting ligand in this study. Incorporation of biologically active cRGD peptide on the surface of nanoparticles was confirmed by *in vitro* cell uptake studies and *in vivo* tumor accumulation studies. Functionalization of nanoparticles with cRGD peptide increased the cellular uptake of nanoparticles 2–3-fold, and this enhancement in uptake was substantially reduced by the presence of excess cRGD molecules. In a syngeneic mouse 4T1 tumor model, cRGD functionalization resulted in increased accumulation and retention of nanoparticles in the tumor tissue (nearly 2-fold greater area under the curve), confirming the *in vivo* activity of cRGD functionalized nanoparticles. In conclusion, the IAASF technique enabled the incorporation of reactive maleimide groups on PLGA nanoparticles, which in turn permitted efficient conjugation of biologically active cRGD peptide to the surface of PLGA nanoparticles.

Keywords

Targeted delivery; surface functionalization; chemotherapy; polymeric nanoparticles; peptide ligands

Introduction

Targeted drug delivery has the potential to increase the fraction of administered dose reaching the disease site while minimizing non-specific drug distribution. Delivery systems used for targeting most often comprise of a drug carrier attached to a ligand that binds with a specific target overexpressed at the disease site.[1] Polymeric nanoparticles, especially those

*CORRESPONDING AUTHOR FOOTNOTE: Department of Pharmaceutics, College of Pharmacy, 308 Harvard St., S.E., Minneapolis, MN 55455, Phone: 612-624-0951, Fax: 612-626-2125, jpanyam@umn.edu.

formulated using poly(D,L-lactide-*co*-glycolide) (PLGA) copolymer, have emerged as promising carriers for targeted delivery of a wide variety of payloads.[2] PLGA nanoparticles have the advantages of biocompatibility, biodegradability, ease of formulation, and tunable sustained release properties.[3]

An important drawback with PLGA nanoparticles is the limited types of functional groups available on the surface for conjugation to targeting ligands.[4] To overcome this limitation, PLGA with specific end terminal groups (such as carboxyl) have been used, the rationale being that some of these functional groups could be available on the surface for chemical reaction.[5–7] Other reports have utilized the hydroxyl groups of residual polyvinyl alcohol present on the surface of PLGA nanoparticles after fabrication.[8] Other surfactants with the required functional groups have also been used in the fabrication of nanoparticles, which enables ligand attachment to the surfactant adsorbed on the surface of the particles.[9] A recent report used the diblock copolymer polycaprolactone - polyethylene glycol dissolved along with PLGA to prepare PLGA nanoparticles with PEG on the surface. These nanoparticles were then conjugated to cRGD peptide for tumor targeting.[10]

Recently, we have reported the use of Interfacial Activity Assisted Surface Functionalization (IAASF) technique to introduce polyethylene glycol (PEG) molecules and targeting ligands such as folic acid on the surface of PLGA nanoparticles in a single step.[11] This technique involves the partitioning of polylactide (PLA)-PEG-ligand conjugate at the oil/water interface formed during nanoparticle formulation, resulting in the formation of nanoparticles with PEG-conjugated ligand on the surface of nanoparticles. However, this procedure involves an oil/water interface, and may, therefore, not be suitable for ligands that are sensitive to organic solvents (for example, peptides and proteins).

In the current report, we demonstrate that the IAASF method can be used to incorporate reactive functional groups onto the surface of PLGA nanoparticles. In addition to enabling the introduction of new functional groups, this approach lends itself to more chemoselective bioconjugation approaches.[12] The IAASF strategy differs from previously reported surface functionalization techniques[13,14] in the fact that nanoparticles formed are not micellar but are polymeric matrix-type devices. This enables the incorporation and sustained release of a wide variety of therapeutic agents including proteins and nucleic acids [15–17]. Using the IAASF procedure, we fabricated PLGA nanoparticles with surface maleimide groups, which were then used to attach cRGD peptide to nanoparticles. The cRGD peptide targets $\alpha_v\beta_3$ integrins overexpressed on tumor vasculature and some tumor cells,[10,18,19] and was used as model targeting ligand in this study. Cell culture and mouse tumor model studies confirmed the incorporation of biologically active cRGD peptide molecules on the surface of nanoparticles.

Materials and methods

Materials

PLGA (lactide-to-glycolide ratio of 50:50 and inherent viscosity 0.61 dl/g) was purchased from Absorbable Polymers (Pelham, AL). Bifunctional PEG with hydroxyl and maleimide groups (Mol Wt. 3400 Da; abbreviated as HO-PEG-MAL) was purchased from Laysan Bio Inc. (Arab, AL). cRGDfK-thioacetyl ester [(cRGDfK-(Ac-SCH_2CO)] was purchased from Peptide International Inc. (Louisville, KY). Phosphate buffered saline (PBS), Triton-X 100, chloroform, toluene, methanol, and acetonitrile were obtained from Fisher Scientific (Pittsburgh, PA). Glacial acetic acid was procured from Alfa Aesar (Ward Hill, MA). Polyvinyl alcohol (PVA) (average MW 30,000–70,000 Da), stannous 2-ethyl-hexanoate, and methyl tri-chlorosilane were from Sigma-Aldrich (St Louis, MO). RPMI cell media, fetal

bovine serum, and trypsin were purchased from Invitrogen (Carlsbad, CA). HUVEC media was supplied by AllCells (Emeryville, CA).

Methods

Preparation of PLA-co-PEG maleimide—Block co-polymer PLA-*co*-PEG with maleimide end group (abbreviated as PLA-PEG-MAL) was prepared by ring opening polymerization of lactide in solution phase.[20] HO-PEG-MAL was used as macroinitiator and stannous 2-ethyl-hexanoate was used as the catalyst. Glassware was silanized by rinsing with a 5% methyl tri-chlorosilane solution in toluene, then with acetone, and finally dried overnight at 130 °C. HO-PEG-MAL (90 mg) and L-lactide (460 mg) were placed in a silanized, two-armed round bottom flask, fitted with Dean-Stark apparatus, water condenser, and nitrogen inlet. 30 ml toluene was added to the flask and stirred at 60° C to dissolve the contents. To remove traces of moisture present in PEG, about 70% of the added toluene was removed by distillation under nitrogen atmosphere. 25 mg of stannous 2-ethyl-hexanoate, dissolved in 2 ml toluene, was added to the above reaction mixture and refluxed at 110 °C for 4 hr under nitrogen. The residual solvent was removed under vacuum using a rotary evaporator. The remaining viscous material was heated to 140 °C for 1 hr under nitrogen. The reaction mixture was cooled and dissolved in 10–15 ml dichloromethane. Chilled diethyl ether was then added slowly to the polymer solution under stirring. Polymer was purified by precipitation in dichloromethane-diethyl ether (50/50) mixture, filtered, and dried under vacuum. The final product was characterized by ^{1}H-NMR spectroscopy after dissolving the polymer in deuterated chloroform (800 MHz, Varian INOVA). A ^{1}H peak at δ =1.5 related to CH_3 group of PLA, peak at δ= 5.2 corresponding to -CH- of PLA backbone and peak at δ= 3.6 corresponding to -CH_2- of PEG in the proton NMR spectrum confirmed the formation of the copolymer[21] (NMR spectra not shown). Molecular weight of the co-polymer was determined by gel permeation chromatography (GPC). A Waters 717 Plus autosampler connected to a Waters 590 programmable HPLC pump, ultraviolet-visible and refractive index detectors was used. Tetrahydrofuran was used as the mobile phase at a flow rate of 1 ml/min. Molecular weight of the polymer measured by GPC was 13.4 kDa.

Preparation of maleimide functionalized PLGA nanoparticles—PLGA (30 mg) and 6-coumarin (250 μg) were dissolved in 1 ml chloroform. An oil-in-water emulsion was formed by emulsifying the polymer solution in 8 ml of 2.5% w/v aqueous PVA solution by probe sonication (18–24 Watt; Sonicator® XL, Misonix, NY) for 5 minutes over an ice bath. The diblock copolymer PLA-PEG-MAL (8 mg) was dissolved in chloroform (200 μl) and added drop-wise to the above emulsion with stirring. The emulsion was stirred for 18 hrs at ambient conditions followed by 2 hrs under vacuum to remove the residual chloroform. Nanoparticles were recovered by ultracentrifugation (35,000 rpm for 35 min at 4 °C, Optima™ LE-80K, Beckman, Palo Alta, CA) and washed three times with deionized water. Nanoparticle suspension was then lyophilized (Labconco, FreeZone 4.5, Kansas City, MO) to obtain a dry powder. 6-Coumarin is a highly lipophilic molecule that has been used by several groups as a marker for polymeric nanoparticles.[22–26] Previous studies have shown that less than 0.1% of the encapsulated molecule is released in 48 hrs.[24]

Conjugation of cRGD and cRAD peptides to maleimide functionalized PLGA nanoparticles—cRGD or cRAD peptide conjugated nanoparticles were prepared by reacting 40 mg of maleimide functionalized nanoparticles with 4 mg of cRGDfK-thioacetyl ester or cRADfK-thioacetyl ester in a 0.05 M HEPES and 0.05 M EDTA solution for 12 hrs at room temperature.[27] The peptides were preincubated in 200 μL of HEPES-EDTA buffer containing 0.005 M hydroxyl amine hydrochloride for 30 min before adding to nanoparticle dispersion. Following peptide conjugation, nanoparticles were washed thrice with HEPES-EDTA solution by repeated ultracentrifugation as described previously. Nanoparticles were

then further dialyzed for 24 hrs against distilled water (40 kDa MWCO, Spectrum Laboratories, Rancho Dominguez, CA) and then lyophilized.

Characterization of nanoparticles—The incorporation of PLA-PEG-MAL in PLGA nanoparticles was determined by ^{1}H NMR. Nanoparticle formulations (10 mg) were dissolved in deuterated chloroform ($CDCl_3$; 1 ml) and analyzed using an 800 MHz NMR instrument. ZetaPlus dynamic light scattering equipment (Brookhaven Instruments, Holtsville, NY) was used for determining both the hydrodynamic diameter and the zeta potential. Nanoparticles (~1 mg/ml) were dispersed in distilled water using sonication prior to analysis. Mean hydrodynamic diameters were calculated based on size distribution by weight assuming a lognormal distribution, and the results were expressed as mean particle size, along with d_{10} (equivalent diameter where 10 mass-% of the particles have a smaller diameter) and d_{90} (equivalent diameter where 90 mass-% of the particles has a smaller diameter). Zeta potential values were calculated from measured velocities using Smoluchowski's equation, and results were expressed as mean ± S.E.M. of five runs. 6-coumarin loading in nanoparticles was determined by extraction from a known amount of nanoparticles with methanol for 12 hrs. Samples were centrifuged and analyzed by HPLC for 6-coumarin concentration using a modification of a previously reported method.[23] A Beckman Coulter HPLC system (Fullerton, CA) equipped with System Gold 125 solvent module, System Gold 508 auto-injector, System Gold 168 PDA UV/Visible detector, FP-2020 plus fluorescence detector (JASCO Inc., Easton, MD), and a C-8 ODS column (4.6 × 250 mm; 4 μm particle size, Beckman Coulter) was used. Mobile phase consisting of acetonitrile and 1-heptane sulfonate (1 g/L) (75:25 ratio) was used at a flow rate of 1 ml/min. The retention time of 6-coumarin was around 5 minutes. The number of peptide molecules in a known weight of nanoparticles was determined using a commercially available BCA protein assay kit (Pierce). Nanoparticles without peptide functionalization were used to correct for background absorbance. Based on the particle size and density of the polymer, 1 mg of nanoparticles was estimated to contain ~10^{12} particles. The results were expressed as the average (± S.D.) number of peptide molecules present on each particle.

NMR confirmation of cRGD peptide conjugation to PLA-PEG-MAL micelles—About 100 mg of PLA-PEG-MAL was dissolved in 1 ml DMSO. To this, a reaction buffer consisting of 0.05 M HEPES and 0.05 M EDTA was added drop-wise until the solution became milky, indicating the formation of fine colloidal particles. The cRGD peptide was then conjugated to the particles using reaction conditions similar to that for maleimide functionalized nanoparticles. Following overnight reaction, the reaction mixture was diluted with 10 ml of reaction buffer and then dialyzed for 6 hrs against reaction buffer and 24 hrs against distilled water at 4 °C (500 Da MWCO). The dialysis medium outside the dialysis bag was changed twice. The polymer sample was then freeze dried. ^{1}H NMR was recorded by dissolving 10 mg of the sample in 1 ml of $CDCl_3$.

Effect of cRGD functionalization on cellular uptake of nanoparticles—NCI/ADR-RES, MCF-7, and 4T1 cells were used as model tumor cells, while human umbilical vein endothelial cells (HUVEC) were used as model endothelial cells. NCI-ADR, MCF-7, and 4T1 cells were cultured in RPMI-1640 Glutamax® medium containing 10% fetal bovine serum and HUVEC was cultured in HUVEC medium containing 10% growth supplements. Cells were maintained at 37 °C and 5% CO_2. For uptake studies, cells were seeded in a 24-well plate at 50,000 cells/well seeding density and allowed to attach for 48 hrs. Cells were treated with nanoparticles with or without cRGD surface functionalization, with cRAD surface functionalization, and in the presence or absence of 10-fold excess of cRGD peptide for 30 min. Cells were then washed with PBS and lysed using 1% w/v Triton X-100 in 8

mM potassium phosphate buffer. A part of the cell lysate was lyophilized and extracted with methanol. The 6-coumarin concentration in the methanol extracts was determined by HPLC analysis. Nanoparticle concentration in the cell lysate was normalized to the total cell protein determined using Pierce protein assay kit.

Effect of cRGD functionalization on cellular retention of nanoparticles—A previously reported exocytosis assay [28] was used to study the effect of cRGD functionalization on retention of nanoparticles in NCI/ADR-RES cells. Cells were seeded in 24 well plates at a density of 25,000/well and allowed to attach for 24 hrs. Cells were then treated with nanoparticles (100 μg/well). After incubation for 30 min at 37 °C, cells were washed twice with PBS and further incubated with regular culture medium. A set of cells was washed at different time intervals and lysed. Concentration of nanoparticles in the cell lysate was determined using HPLC as described above.

Effect of cRGD functionalization on tumor accumulation of nanoparticles—All the experiments involving animals were approved by the Institutional Animal Care and Use Committee of the University of Minnesota. 4T1 tumors were induced in 6–8 week old female BALB/c mice (Charles River, MA) by subcutaneous injection of about 500,000 cells dispersed in PBS on the dorsal side. Tumors were measured using Vernier calipers every alternate day. When tumors reached a volume of ~150 mm^3, nanoparticles (1 mg/animal, suspended in 100 μl of PBS) were injected through the tail vein. Mice were euthanized at 3, 6, and 24 hours after injection. To quantify the amount of nanoparticles that accumulated in tumor, the tissue was homogenized, lyophilized, and extracted overnight with diethyl ether. Extracted samples were centrifuged and 1 ml of the supernatant was evaporated. Samples were reconstituted in 500 μl methanol and analyzed for 6-coumarin concentration using HPLC as described earlier. 6-coumarin loading information was used to determine the nanoparticle amount and the data was normalized to the wet weight of tissue. The area under the curve (AUC) of tumor concentration (C) - time profile was calculated using the trapezoidal rule as follows:

$$AUC_{0-24}=AUC_{0-3}+AUC_{3-6}+AUC_{6-24}$$
$$AUC_1=\frac{C_0+C_1}{2}*Time_{1-0}$$

where C_0 and C_1 are tumor concentrations of nanoparticles at time T_0 and T_1.

Statistical analysis—One-way ANOVA was used for comparisons involving more than two groups. Student's t-test was used for comparisons involving two groups. A probability level of $P < 0.05$ was considered significant.

Results and Discussion

Preparation and characterization of cRGD and cRAD conjugated PLGA nanoparticles

In the current study, we evaluated the use of the IAASF technique to incorporate reactive maleimide groups on the surface of PLGA nanoparticles. The IAASF technique utilizes the differential behavior of the hydrophobic and hydrophilic segments of a block copolymer at the oil/water interface.[11] The hydrophobic block partitions into the organic phase while the hydrophilic block remains in the aqueous phase.[29] Thus, when a copolymer like PLA-PEG with a terminal maleimide group is added to the polymer emulsion formed as a part of the nanoparticle fabrication process, the copolymer spontaneously localizes and orients itself at the oil/water interface. The PLA block partitions into the chloroform phase containing PLGA polymer while PEG block remains in the aqueous phase. Removal of chloroform by

evaporation results in the formation of PLGA nanoparticles with PEG and reactive functional groups on the surface of nanoparticles (Figure 1).

There are several advantages to this novel surface functionalization approach. IAASF technique depends only on the interfacial activity of the block copolymer and the presence of oil/water interface. The method can, therefore, be potentially used for a wide variety of polymers and functional groups. Further, this approach is suitable for encapsulation and sustained release of drugs, proteins, and nucleic acids. Importantly, IAASF technique can be used to incorporate multiple functional groups on the nanoparticle surface in a single step. To demonstrate the proof-of-concept, the IAASF technique was used to incorporate maleimide groups on the surface of PLGA nanoparticles.

Nanoparticles with maleimide groups on the surface were reacted with cRGDfK-thioacetyl ester (Figure 1). The thioacetyl ester was hydrolyzed to -$COCH_2SH$ using hydroxyl amine. ^1H peak at ~ 3.6 ppm corresponding to -OCH_2–CH_2- of PEG (arrow in Figure 2A) confirmed the presence of PLA-PEG-MAL in nanoparticles. Control nanoparticles formulated without PLA-PEG functionalization did not have this peak. Possibly due to the low molar ratio of cRGD compared to that of PLGA in nanoparticles and interference from $CDCl_3$ peak, we did not observe a distinct aromatic peak around 7.2 ppm related to the aromatic protons of phenylalanine present in the cRGD sequence. However, to confirm the feasibility of the reaction, we prepared micelles of PLA-PEG-MAL and then reacted the micelles with c[RGDfK]$COCH_2SH$. Disappearance of the prominent ^1H peak related to maleimide at 6.6 ppm confirmed the completion of the reaction (Figures 2B & 2C). A similar disappearance of ^1H peak related to maleimide in the NMR spectrum was used recently as a positive confirmation of cRGD conjugation to PLA-PEG micelles.[30] BCA protein assay indicated that about 4.5 ± 0.8 μg of cRGD and 7.1 ± 0.4 μg of cRAD peptides were conjugated per mg of cRGD functionalized and cRAD functionalized nanoparticles, respectively. Based on the assumption of 10^{12} nanoparticles/mg, the peptide content translates into 3,877 ± 704 cRGD molecules or 5,862 ± 369 cRAD molecules conjugated to each nanoparticle.

Particle size and surface charge are important determinants of nanoparticle behavior in biological systems.[31] Dynamic light scattering studies indicated that nanoparticles had a mean hydrodynamic diameter of ~210 nm (Table 1). The particle size and distribution was not affected significantly by peptide conjugation (Table 1 and Figure 3). The surface charge of non-functionalized nanoparticles was about −40 mV; cRGD functionalization reduced the surface charge but the particles were still strongly anionic (Table 1). 6-coumarin (fluorescent label) loading in nanoparticles before cRGD conjugation was 0.59% w/w and was 0.52% w/w post-conjugation. Thus, cRGD conjugation did not result in significant changes in nanoparticle characteristics that might influence their efficacy.

Cell uptake studies

It has been previously shown that the cRGD peptide increases the cellular uptake of nanocarrier systems by targeting the $\alpha_v\beta_3$ integrin.[10,18,19] To confirm the activity of cRGD molecules conjugated to the surface of PLGA nanoparticles, *in vitro* cell uptake studies were carried out with fluorescently-labeled cRGD nanoparticles in 4T1 cells. Nanoparticles that were functionalized with a non-targeted peptide (cRAD) and nanoparticles without peptide functionalization (nanoparticles with maleimide groups) were used as controls. cRGD functionalization significantly increased the uptake of nanoparticles ($P < 0.05$; Figure 4). Functionalization with the non-targeted cRAD peptide did not enhance nanoparticle uptake. Addition of excess cRGD molecules competitively decreased the cellular uptake of cRGD functionalized nanoparticles but not of control nanoparticles or cRAD-functionalized nanoparticles, indicating that the mechanism of cellular uptake was different for targeted and

non-targeted nanoparticles. These results suggest that specific receptors could be involved in the uptake of cRGD functionalized nanoparticles but not in that of non-targeted nanoparticles.[10]

Fluorescence microscopy was used to verify that nanoparticles were internalized into the cells and not simply bound to the cell surface. As can be seen in Figure 5, nanoparticle-associated green fluorescence was seen inside the cells and was often co-localized with red fluorescence from LysoTracker Red®. The co-localization (shown as yellow fluorescence in the overlays) of nanoparticles with a marker for endo-lysosomes clearly indicate that nanoparticles are taken up into the cells, likely through the endocytic pathway [15].

To confirm that enhanced cellular uptake of cRGD-functionalized nanoparticles was not limited to one cell line, we evaluated nanoparticle uptake in various cell lines. As the cellular uptake of non-functionalized nanoparticles were similar to that cRAD functionalized nanoparticles (see above), non-functionalized nanoparticles were used as controls in these studies. Functionalization with cRGD enhanced nanoparticle uptake in all cell lines studied (Figure 6). The degree of enhancement of nanoparticle uptake varied from about 2- to 3-fold, depending on the cell line. This variation may be the result of many factors including the expression level of the $\alpha_v\beta_3$ integrins and the rate of endocytosis in the different cell lines.[32]

A dose response study was performed to evaluate if cRGD functionalization enabled greater cell uptake of nanoparticles at different doses. Figure 7 shows that cRGD functionalized nanoparticles were taken up to a greater extent than non-functionalized nanoparticles at all doses studied. However, the difference in cellular accumulation between ligand-functionalized and control nanoparticles appear to diminish at high doses, potentially because of saturation of available receptors for cRGD peptide.

Previous studies have shown that following uptake into cells through endocytosis, nanoparticles reach the recycling endosomes, from where a fraction is recycled back to the cell's exterior, while the other fraction advances to secondary endosomes and lysosomes.[33] If the concentration of nanoparticles outside the cell is maintained, the recycling continues, resulting in steady state intracellular concentration of nanoparticles. However, if the concentration outside the cell declines, the recycling is disrupted and results in a decrease in the intracellular concentration of nanoparticles. To study the effect of cRGD functionalization on the intracellular retention of nanoparticles, NCI/ADR-RES cells were incubated with cRGD functionalized and non-functionalized nanoparticles for 30 min, washed, and the incubations were continued in cell culture medium. As shown in Figure 8, once the nanoparticles were removed from the external medium, intracellular concentration of nanoparticles declined for both cRGD functionalized and non-functionalized nanoparticles. It is important to note that, despite the overall decline, cRGD functionalization resulted in higher nanoparticle amounts in cells relative to non-functionalized nanoparticles at the end of the experiment. Overall, these cellular uptake studies showed that cRGD molecules present on the surface of nanoparticles were biologically active and can recognize the intended target.

In vivo tumor accumulation studies

Tumor targeting of cRGD functionalized and control nanoparticles following intravenous administration was studied in a syngeneic 4T1 tumor model. Tumor concentration-time profiles of nanoparticles are shown in Figure 9. Functionalization with the cRGD peptide resulted in a significant increase in nanoparticle exposure in the tumor tissue. The area under the curve (AUC) for cRGD functionalized nanoparticles in the tumor was nearly 2-fold higher than that for non-functionalized nanoparticles (100 Vs 60 μg.hr/mg). It is important

to note that in the case of cRGD functionalized nanoparticles, concentration in the tumor remained high for up to 24 hrs. With non-functionalized nanoparticles, concentration in the tumor increased slowly over 6 hrs and then declined through 24 hrs. About 24 hrs post injection, tumor accumulation of cRGD functionalized nanoparticles was almost 4-fold higher than that of non-functionalized nanoparticles.

Previous studies have shown that colloidal carriers accumulate in tumors through the enhanced permeation and retention (EPR) effect, which arises as a result of the leaky vasculature and poorly developed lymphatics in tumors.[34] Incorporation of targeting ligands enables the binding of the carrier with specific targets in the tumor tissue, resulting in enhanced EPR effect and higher intratumoral accumulation.[35] Our *in vitro* studies showed that cRGD functionalization resulted in greater internalization and longer retention of nanoparticles within tumor epithelial and microvascular endothelial cells. These interactions could have resulted in increased accumulation and retention of cRGD functionalized nanoparticles in the tumor. No such interactions were possible for non-functionalized nanoparticles, resulting in slow accumulation and rapid decline of control nanoparticles, and an overall decrease in nanoparticle exposure in the tumor tissue. Considering the fact that PLGA nanoparticles release their payload over a period of weeks,[36] the longer residence time of cRGD functionalized nanoparticles in tumor will help increase the anticancer efficacy of the payload. The present study thus shows the potential of the IAASF technique to enable the incorporation of reactive functional groups and the conjugation of peptide ligands on the surface of PLGA nanoparticles. Studies investigating the anticancer efficacy of drug-loaded, cRGD functionalized nanoparticles in different tumor models are in progress.

Conclusion

The IAASF methodology enabled the incorporation of maleimide functional groups on the surface of PLGA nanoparticles, which in turn permitted efficient conjugation of cRGD peptide to the nanoparticles. cRGD functionalization significantly enhanced nanoparticle accumulation in tumor cells *in vitro* and resulted in improved tumor accumulation of nanoparticles in a mouse model. We expect that the IAASF technique can be adapted to incorporate other functional groups as well, which will further expand the usefulness of PLGA nanoparticles in targeted drug delivery.

Acknowledgments

Funding from NIH (7R21CA116641). We thank Mr. Zhengxi Zhu (Department of Chemical Engineering & Materials Science, University of Minnesota) for his help in obtaining DLS and GPC data. We thank the University of Minnesota BioMedical NMR Resource with instrumentation provided by funds from the NSF (BIR-961477), the University of Minnesota Medical School, and the Minnesota Medical Foundation and Mr. Todd Rappe for help with NMR data collection and processing. We also thank Brenda Koniar and Angela Blum (Research Animal Resources, University of Minnesota) for assistance with the animal studies.

References

1. Suri SS, Fenniri H, Singh B. Nanotechnology-based drug delivery systems. J Occup Med Toxicol. 2007; 2:16. [PubMed: 18053152]
2. Lu JM, Wang X, Marin-Muller C, Wang H, Lin PH, Yao Q, Chen C. Current advances in research and clinical applications of PLGA-based nanotechnology. Expert Rev Mol Diagn. 2009; 9:325–341. [PubMed: 19435455]
3. Panyam J, Labhasetwar V. Sustained cytoplasmic delivery of drugs with intracellular receptors using biodegradable nanoparticles. Mol Pharm. 2004; 1:77–84. [PubMed: 15832503]
4. Mohamed F, van der Walle CF. Engineering biodegradable polyester particles with specific drug targeting and drug release properties. J Pharm Sci. 2008; 97:71–87. [PubMed: 17722085]

5. McCarron PA, Marouf WM, Donnelly RF, Scott C. Enhanced surface attachment of protein-type targeting ligands to poly(lactide-co-glycolide) nanoparticles using variable expression of polymeric acid functionality. J Biomed Mater Res A. 2008; 87:873–884. [PubMed: 18228271]
6. McCarron PA, Marouf WM, Quinn DJ, Fay F, Burden RE, Olwill SA, Scott CJ. Antibody targeting of camptothecin-loaded PLGA nanoparticles to tumor cells. Bioconjug Chem. 2008; 19:1561–1569. [PubMed: 18627195]
7. Kocbek P, Obermajer N, Cegnar M, Kos J, Kristl J. Targeting cancer cells using PLGA nanoparticles surface modified with monoclonal antibody. J Control Release. 2007; 120:18–26. [PubMed: 17509712]
8. Sahoo SK, Labhasetwar V. Enhanced antiproliferative activity of transferrin-conjugated paclitaxel-loaded nanoparticles is mediated via sustained intracellular drug retention. Mol Pharm. 2005; 2:373–383. [PubMed: 16196490]
9. Keegan ME, Royce SM, Fahmy T, Saltzman WM. In vitro evaluation of biodegradable microspheres with surface-bound ligands. J Control Release. 2006; 110:574–580. [PubMed: 16386325]
10. Danhier F, Vroman B, Lecouturier N, Crokart N, Pourcelle V, Freichels H, Jerome C, Marchand-Brynaert J, Feron O, Preat V. Targeting of tumor endothelium by RGD-grafted PLGA-nanoparticles loaded with Paclitaxel. J Control Release. 2009; 140:166–173. [PubMed: 19699245]
11. Patil YB, Toti US, Khdair A, Ma L, Panyam J. Single-step surface functionalization of polymeric nanoparticles for targeted drug delivery. Biomaterials. 2009; 30:859–866. [PubMed: 19019427]
12. Beaudette TT, Cohen JA, Bachelder EM, Broaders KE, Cohen JL, Engleman EG, Fréchet JMJ. Chemoselective Ligation in the Functionalization of Polysaccharide-Based Particles. J Am Chem Soc. 2009; 131:10360–10361. [PubMed: 19591467]
13. Farokhzad OC, Jon S, Khademhosseini A, Tran TNT, LaVan DA, Langer R. Nanoparticle-Aptamer Bioconjugates: A New Approach for Targeting Prostate Cancer Cells. Cancer Res. 2004; 64:7668–7672. [PubMed: 15520166]
14. Gu F, Zhang L, Teply BA, Mann N, Wang A, Radovic-Moreno AF, Langer R, Farokhzad OC. Precise engineering of targeted nanoparticles by using self-assembled biointegrated block copolymers. Proc Natl Acad Sci. 2008; 105:2586–2591. [PubMed: 18272481]
15. Panyam J, Zhou WZ, Prabha S, Sahoo SK, Labhasetwar V. Rapid endo-lysosomal escape of poly(DL-lactide-co-glycolide) nanoparticles: implications for drug and gene delivery. FASEB J. 2002; 16:1217–1226. [PubMed: 12153989]
16. Sahoo SK, Ma W, Labhasetwar V. Efficacy of transferrin-conjugated paclitaxel-loaded nanoparticles in a murine model of prostate cancer. Int J Cancer. 2004; 112:335–340. [PubMed: 15352049]
17. Sun B, Ranganathan B, Feng SS. Multifunctional poly(D,L-lactide-co-glycolide)/montmorillonite (PLGA/MMT) nanoparticles decorated by Trastuzumab for targeted chemotherapy of breast cancer. Biomaterials. 2008; 29:475–486. [PubMed: 17953985]
18. Castel S, Pagan R, Mitjans F, Piulats J, Goodman S, Jonczyk A, Huber F, Vilaro S, Reina M. RGD peptides and monoclonal antibodies, antagonists of alpha(v)-integrin, enter the cells by independent endocytic pathways. Lab Invest. 2001; 81:1615–1626. [PubMed: 11742032]
19. Dubey PK, Mishra V, Jain S, Mahor S, Vyas SP. Liposomes modified with cyclic RGD peptide for tumor targeting. J Drug Target. 2004; 12:257–264. [PubMed: 15512776]
20. Nasongkla N, Bey E, Ren J, Ai H, Khemtong C, Guthi JS, Chin SF, Sherry AD, Boothman DA, Gao J. Multifunctional polymeric micelles as cancer-targeted, MRI-ultrasensitive drug delivery systems. Nano Lett. 2006; 6:2427–2430. [PubMed: 17090068]
21. Li F, Li S, Ghzaoui AE, Nouailhas H, Zhuo R. Synthesis and gelation properties of PEG-PLA-PEG triblock copolymers obtained by coupling monohydroxylated PEG-PLA with adipoyl chloride. Langmuir. 2007; 23:2778–2783. [PubMed: 17243742]
22. Qaddoumi MG, Ueda H, Yang J, Davda J, Labhasetwar V, Lee VH. The characteristics and mechanisms of uptake of PLGA nanoparticles in rabbit conjunctival epithelial cell layers. Pharm Res. 2004; 21:641–648. [PubMed: 15139521]

23. Panyam J, Sahoo SK, Prabha S, Bargar T, Labhasetwar V. Fluorescence and electron microscopy probes for cellular and tissue uptake of poly(D,L-lactide-co-glycolide) nanoparticles. Int J Pharm. 2003; 262:1–11. [PubMed: 12927382]
24. Davda J, Labhasetwar V. Characterization of nanoparticle uptake by endothelial cells. Int J Pharm. 2002; 233:51–59. [PubMed: 11897410]
25. Gao X, Chen J, Tao W, Zhu J, Zhang Q, Chen H, Jiang X. UEA I-bearing nanoparticles for brain delivery following intranasal administration. Int J Pharm. 2007; 340:207–215. [PubMed: 17499948]
26. Zhao J, Liu CS, Yuan Y, Tao XY, Shan XQ, Sheng Y, Wu F. Preparation of hemoglobin-loaded nano-sized particles with porous structure as oxygen carriers. Biomaterials. 2007; 28:1414–1422. [PubMed: 17126898]
27. Nasongkla N, Bey E, Ren J, Ai H, Khemtong C, Guthi JS, Chin SF, Sherry AD, Boothman DA, Gao J. Multifunctional polymeric micelles as cancer-targeted, MRI-ultrasensitive drug delivery systems. Nano Lett. 2006; 6:2427–2430. [PubMed: 17090068]
28. Panyam J, Labhasetwar V. Dynamics of endocytosis and exocytosis of poly(D,L-lactide-co-glycolide) nanoparticles in vascular smooth muscle cells. Pharm Res. 2003; 20:212–220. [PubMed: 12636159]
29. Panyam J, Labhasetwar V. Biodegradable nanoparticles for drug and gene delivery to cells and tissue. Adv Drug Deliv Rev. 2003; 55:329–347. [PubMed: 12628320]
30. Zhan C, Gu B, Xie C, Li J, Liu Y, Lu W. Cyclic RGD conjugated poly(ethylene glycol)-co-poly(lactic acid) micelle enhances paclitaxel anti-glioblastoma effect. J Control Release. 2010; 143:136–142. [PubMed: 20056123]
31. Ratzinger G, Langer U, Neutsch L, Pittner F, Wirth M, Gabor F. Surface Modification of PLGA Particles: The Interplay between Stabilizer, Ligand Size, and Hydrophobic Interactions. Langmuir. 2009
32. Meyer T, Marshall JF, Hart IR. Expression of alphav integrins and vitronectin receptor identity in breast cancer cells. Br J Cancer. 1998; 77:530–536. [PubMed: 9484807]
33. Panyam J, Zhou WZ, Prabha S, Sahoo SK, Labhasetwar V. Rapid endo-lysosomal escape of poly(DL-lactide-co-glycolide) nanoparticles: implications for drug and gene delivery. FASEB J. 2002; 16:1217–1226. [PubMed: 12153989]
34. Wang X, Yang L, Chen ZG, Shin DM. Application of nanotechnology in cancer therapy and imaging. CA Cancer J Clin. 2008; 58:97–110. [PubMed: 18227410]
35. Torchilin VP. Targeted pharmaceutical nanocarriers for cancer therapy and imaging. AAPS J. 2007; 9:E128–147. [PubMed: 17614355]
36. Panyam J, Dali MM, Sahoo SK, Ma W, Chakravarthi SS, Amidon GL, Levy RJ, Labhasetwar V. Polymer degradation and in vitro release of a model protein from poly(D,L-lactide-co-glycolide) nano- and microparticles. J Control Release. 2003; 92:173–187. [PubMed: 14499195]

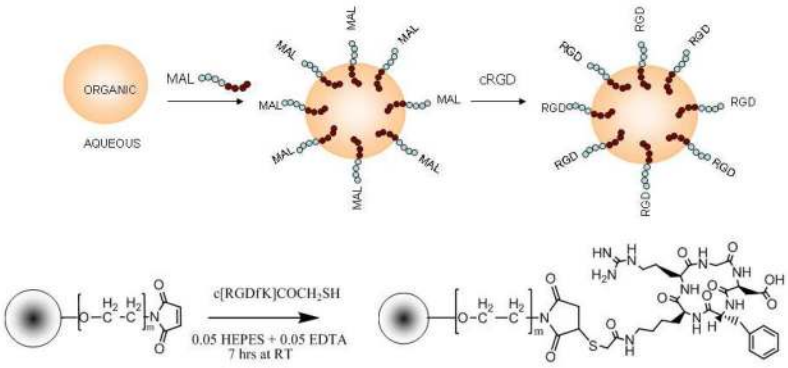

Figure 1.

The IAASF technique (top panel) and the synthetic scheme for conjugation of cRGD peptide to PLGA nanoparticles that are surface functionalized with maleimide groups (bottom panel). PLA-PEG-MAL block copolymer orients itself at the oil-water interface such that PEG molecules are present on the surface of PLGA nanoparticles. Maleimide is then reacted with the cRGD peptide to create cRGD functionalized nanoparticles.

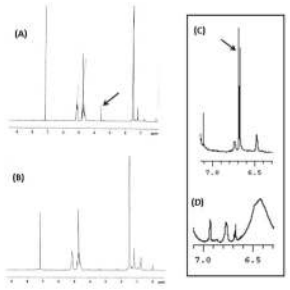

Figure 2.
Proton NMR spectra of (A) nanoparticles with cRGD attached to the surface through PLA-PEG-MAL copolymer; (B) nanoparticles without PLA-PEG-MAL functionalization; (C) proton peak corresponding to the maleimide group in PLA-PEG-MAL polymer micelles and (D) disappearance of the proton peak from the maleimide group following cRGD conjugation to PLA-PEG-MAL micelles.

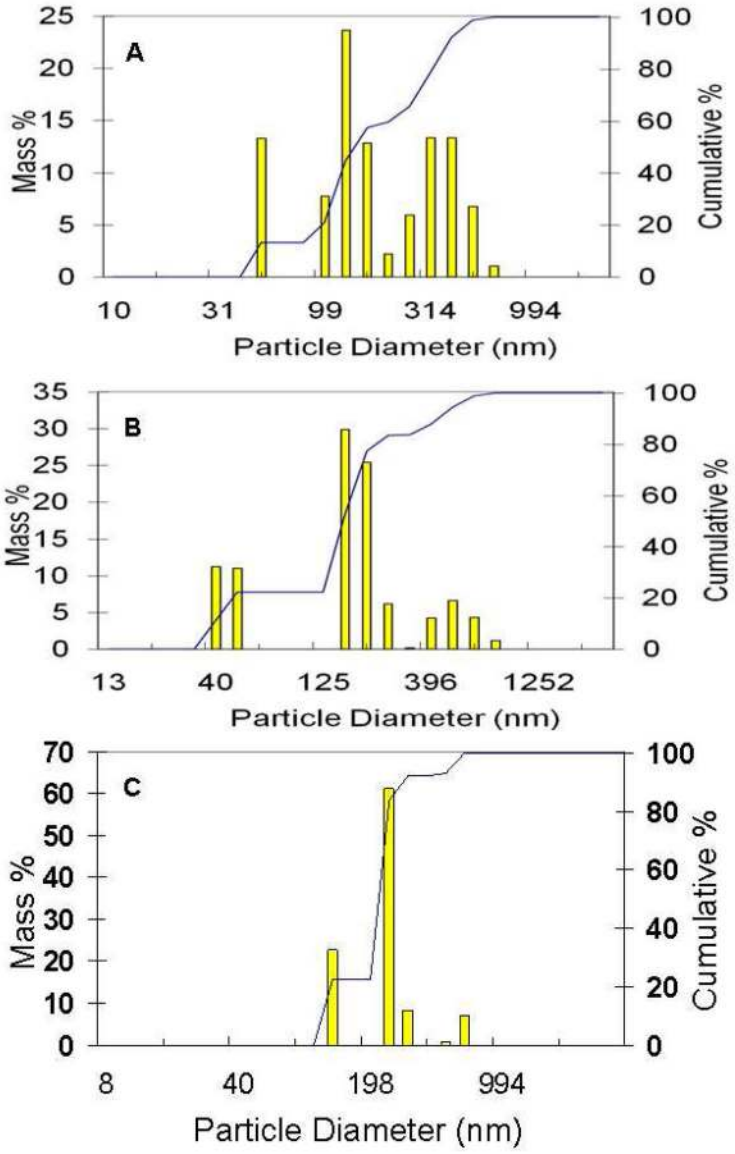

Figure 3.
Particle size distribution of control (A), cRGD functionalized (B) and cRAD functionalized (C) nanoparticles measured by dynamic light scattering.

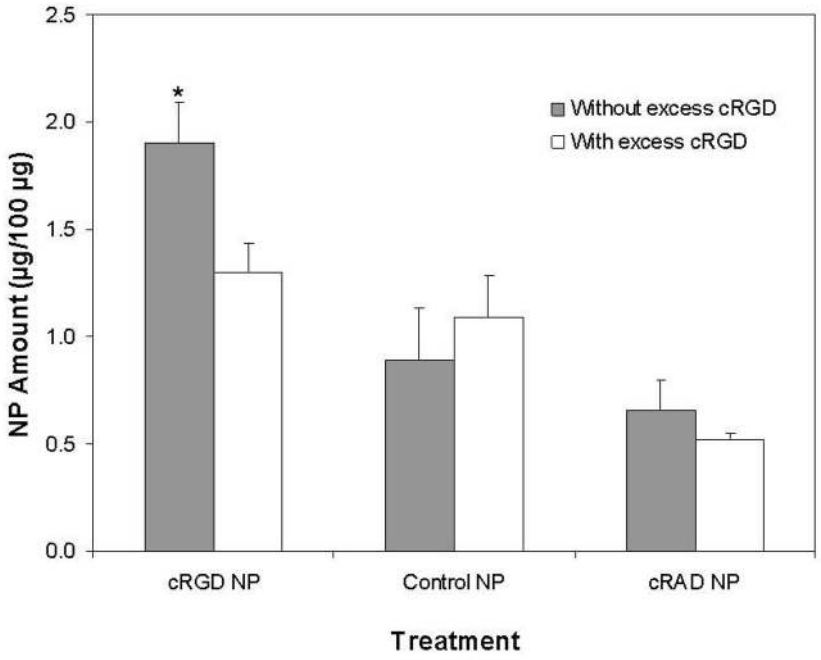

Figure 4.

Effect of cRGD functionalization on nanoparticle accumulation in 4T1 cells. Cells were grown on 24-well plates and incubated with nanoparticles with or without cRGD functionalization (cRGD NP and Control NP, respectively) or with cRAD peptide functionalization (cRAD NP). Nanoparticle amount was determined by HPLC and the data was normalized to the total cell protein. Data as mean ± S.D. (n = 6). *$P < 0.05$ vs. control and cRAD functionalized nanoparticles and cRGD nanoparticles with excess cRGD peptide.

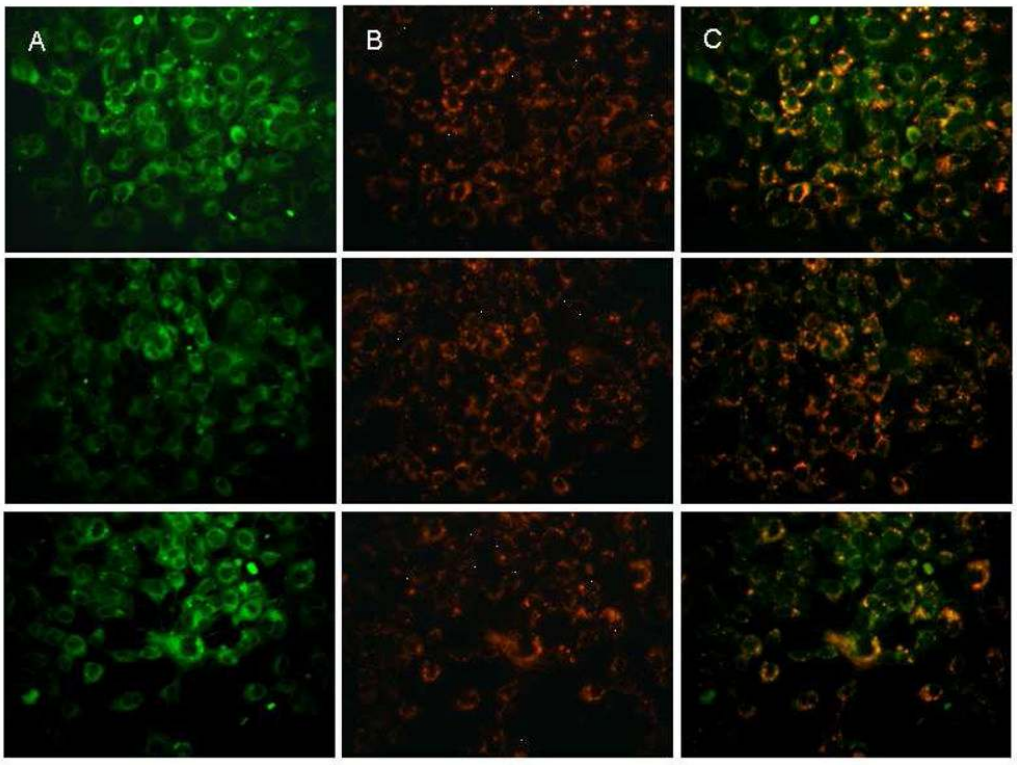

Figure 5.
Nanoparticle uptake in 4T1 cells visualized by fluorescence microscopy. Cells were grown on 8-chamber slides and treated with nanoparticles with cRGD functionalization (top row), with cRAD peptide functionalization (middle row) or nanoparticles without peptide functionalization (bottom row). Cells were imaged 1 hr after nanoparticle incubation, following counterstaining for endo-lysosomes using LysoTracker® Red. Panel A – green fluorescence from nanoparticles; Panel B – red fluorescence from LysoTracker red; and Panel C – merged pictures from red and green filters

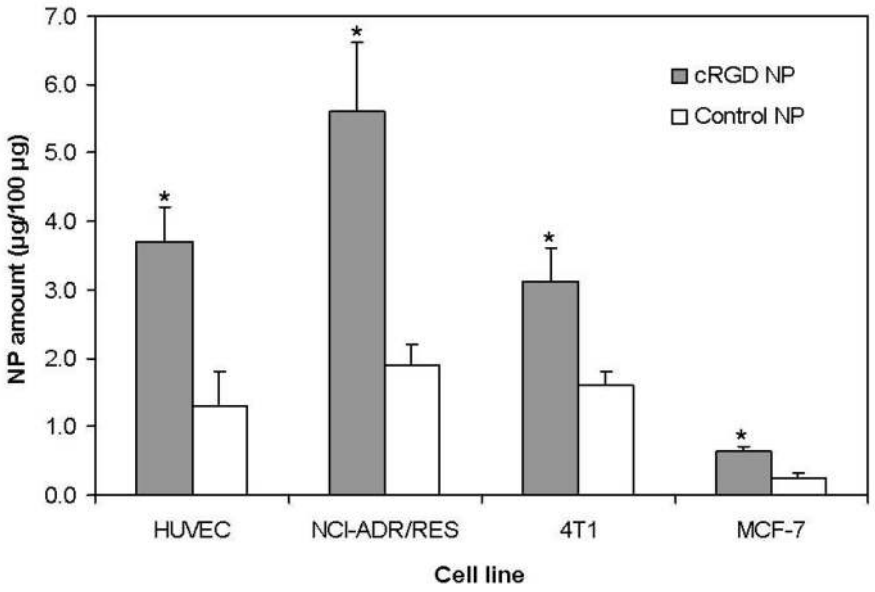

Figure 6.

Effect of cell type on cellular uptake of cRGD functionalized nanoparticles. NCI-ADR/RES, 4T1, MCF-7 or HUVE cells were grown on 24-well plates and incubated with nanoparticles with or without cRGD functionalization (cRGD NP and Control NP, respectively). Nanoparticle amount was determined by HPLC and the data was normalized to the total cell protein. Data as mean ± S.D. (n = 6). *P < 0.05.

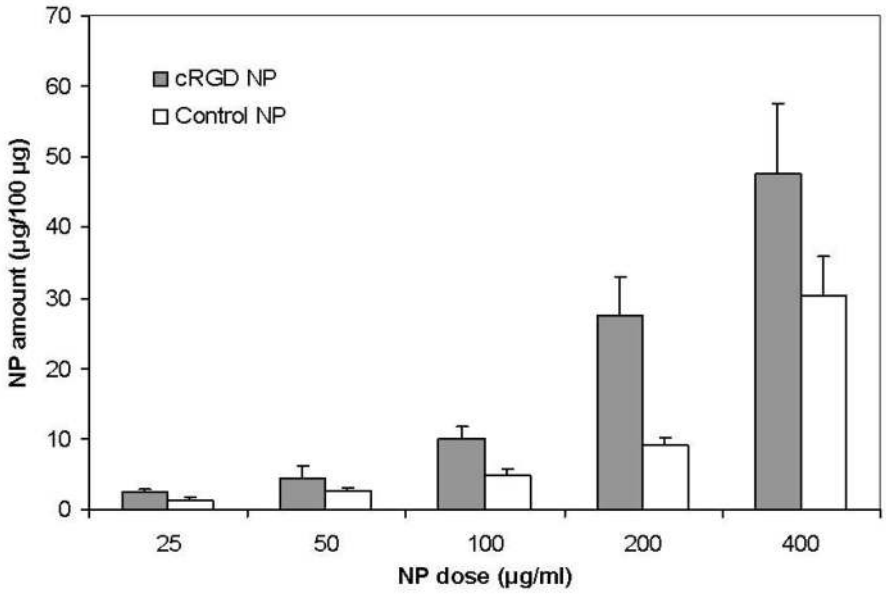

Figure 7.

Effect of nanoparticle dose on the accumulation of nanoparticles with and without cRGD functionalization (cRGD NP and Control NP, respectively) in 4T1 cells. Cells were grown on 24-well plates and incubated with different concentrations of cRGD NP and Control NP. Nanoparticle amount was determined by HPLC and the data was normalized to the total cell protein. Data as mean ± S.D. (n = 6). $P < 0.05$ for all doses.

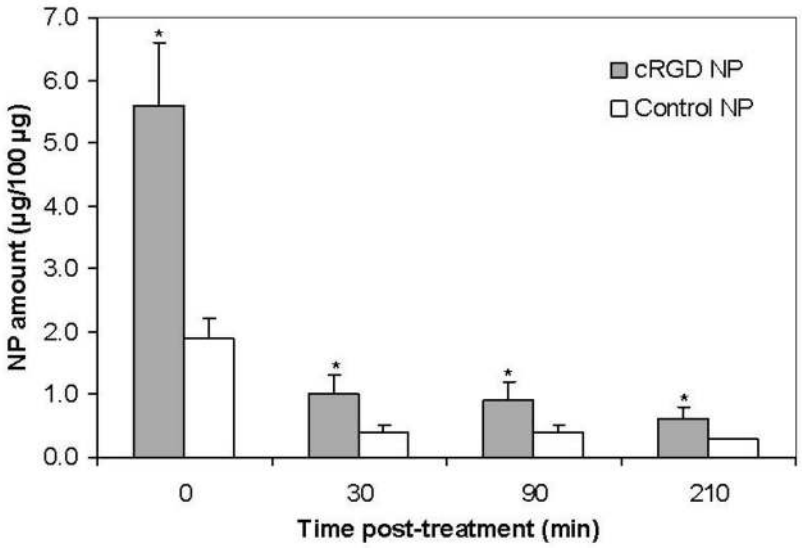

Figure 8.

Effect of cRGD functionalization on nanoparticle retention in NCI-ADR/RES cells. Cells were treated with nanoparticles with or without cRGD functionalization (cRGD NP and Control NP, respectively) for 30 min, washed twice and incubated with fresh medium (0 h time point). Medium was removed and cells were washed and analyzed for nanoparticle levels at different time points. Nanoparticle amount was determined by HPLC and the data was normalized to the total cell protein. Data as mean ± S.D. (n = 6). *P < 0.05.

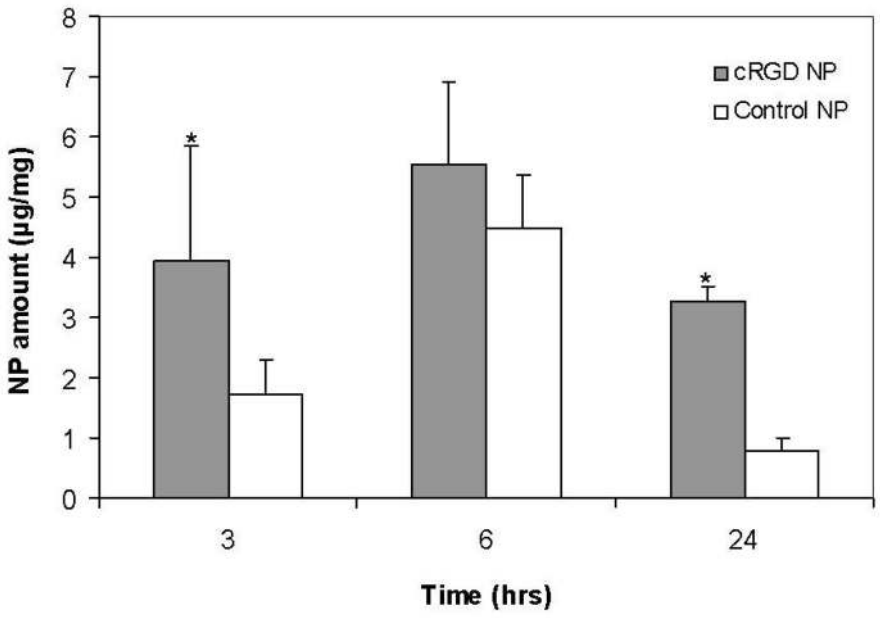

Figure 9.

Effect of cRGD functionalization on tumor accumulation of nanoparticles in BALB/c female mice bearing 4T1 tumors. About 1 mg of nanoparticles with or without cRGD functionalization (cRGD NP and Control NP, respectively) were dispersed in 200 μL PBS and injected through the tail vein. Animals were euthanized 3, 6, and 24 hrs post-injection. Nanoparticle amount was determined by HPLC and the data was normalized to the wet weight of tissue. Data as mean ± S.D. (n = 4). *P < 0.05.

Table 1

Effect of cRGD functionalization on particle size and surface charge of nanoparticles

Formulation	Hydrodynamic diameter (nm)		Zeta potential (mV)
	Mean	d_{10}/d_{90}	
Control NP	217	50/382	− 40.39 ± 0.38
cRGD NP	208	40/428	− 29.12 ± 0.82
cRAD NP	255	111/298	− 19.71 ± 1.42